Proceedings of 20th International Congress on Acoustics, ICA 2010

23–27 August 2010, Sydney, Australia

Acoustic analysis of flat plate trailing edge noise

D.J. Moreau, M.R. Tetlow, L.A. Brooks and C.J. Doolan

School of Mechanical Engineering, The University of Adelaide, Adelaide, SA, 5005 Australia

PACS: 43.28.Ra

ABSTRACT

This paper presents an acoustic analysis of the noise generated at the trailing edge of a flat plate encountering low turbulence fluid flow. Experimental measurements were taken in an anechoic wind tunnel using four microphones: one mounted above the trailing edge, one below the trailing edge, one adjacent to the trailing edge and one above the leading edge. The noise spectra produced by the flat plate were recorded at the four microphone locations. Information about the strength and directivity of the trailing edge noise is determined by comparing the four signals. Subtracting the out-of-phase signals at the microphones above and below the trailing edge is shown to increase the airfoil self-noise spectra further above that of the ambient noise and is shown to be an effective signal extraction technique.

INTRODUCTION

Airfoil self-noise is produced when unsteady flow interacts with an airfoil surface. Trailing edge noise is one of many types of airfoil self-noise (see Brooks et al. (1989)) and is considered to be a major noise generation mechanism in many applications that use airfoil shapes including aircraft, submarines and wind turbines (Blake 1986, Lockard and Lilley 2004, Oerlemans et al. 2009). Designing quiet airfoils to reduce the noise emissions from these applications requires a thorough understanding of the trailing edge noise mechanism and accurate methods of predicting the trailing edge noise radiated into the far-field.

Trailing edge noise is produced when boundary layer turbulence convects past an airfoil trailing edge. Quadrupole noise sources generated by fluid turbulence in the boundary layer are diffracted by the trailing edge and the radiated sound is of dipole nature when the airfoil is acoustically compact ($C << \lambda$, where C is the airfoil chord and λ is the acoustic wavelength). In this case, the sharp trailing edge radiates noise proportional to M^6, where M is the Mach number. For the non compact case ($C >> \lambda$), the radiated sound field exhibits non-multipole behaviour with an amplitude proportional to M^5 (Blake 1986, Doolan 2008). In addition to the broadband noise generated by the interaction of the turbulent boundary layer with the trailing edge, a tonal noise component may be present due to vortex shedding off a blunt trailing edge (Brooks et al. 1989).

A unique characteristic of trailing edge noise is that the sound radiated to opposite sides of the airfoil is correlated, has equal magnitude and a phase difference of 180° (Allen et al. 2002). Two phase-matched microphones located in the far-field, on opposite sides of the airfoil and at the same radial distance from the trailing edge will measure the trailing edge noise to be equal in magnitude and 180° out of phase. Allen et al. (2002), Kunze et al. (2002) and Kunze (2004) used this knowledge to isolate trailing edge noise from background noise sources in far-field acoustic measurements. Experimental results of isolated trailing edge noise obtained with flat plate models at high Reynolds numbers in the experimental study by Kunze et al. (2002) showed some agreement with theoretical predictions of far-field trailing edge noise developed by Howe (1978).

The majority of prediction methods for trailing edge noise have been formulated based on surface pressure fluctuations, including those for example by Chandiramani (1974), Chase (1975), Amiet (1976) and Howe (1978). To determine the accuracy of these prediction methods, a number of experimental studies measuring the airfoil surface pressure distribution and radiated trailing edge noise have been conducted. Brooks and Hodgson (1981) found good agreement between the measured noise spectra for a NACA 0012 airfoil and the noise predicted using measured surface pressure fluctuations and the theory developed by Howe (1978). Schlinker and Amiet (1981) conducted an experimental study of helicopter rotor trailing edge noise, measuring boundary layer and far-field acoustic data for a local blade segment over a range of Mach numbers, propagation angles and airfoil angles of attack. Some agreement was found between measured and predicted noise levels using a generalised description of the surface pressure fluctuations and the theoretical model developed by Amiet (1976). More recently, Roger and Moreau (2004) extended Amiet's (1976) theoretical model to the prediction of trailing edge noise from subsonic fans and found good agreement between experimental data and theory.

As many of the experimental studies conducted in the past have been used to validate theoretical predictions of trailing edge noise based on surface pressure fluctuations, few simultaneous measurements of trailing edge turbulent flow and far-field noise data exist. Experimental data of this kind would provide further insight into the trailing edge noise mechanism and could be used to validate theoretical noise predictions calculated using computational aeroacoustic techniques. Computational aeroacoustic techniques, such as the hybrid LES (Large Eddy Simulation)-acoustic analogy (Khalighi et al. 2010, Wang and Moin 2000, Winkler et al. 2009) or direct compressible LES (Gloerfelt and Le Garrec 2009), calculate far-field noise from direct simulation of the turbulent flow properties and show potential for providing accurate predictions of trailing edge noise.

This paper presents the preliminary results of a larger study to obtain a comprehensive database of experimental trailing edge turbulent flow and far-field noise data for a variety of airfoil shapes. Experimental analysis of trailing edge noise for a flat plate encountering smooth fluid flow is detailed here. The characteristics of trailing edge noise are investigated using far-field acoustic data obtained in the anechoic wind tunnel at the

University of Adelaide. Acoustic spectra and information about the directivity of the trailing edge noise is inferred from four microphones located around the flat plate: one mounted above the trailing edge, one below the trailing edge, one adjacent to the trailing edge and one above the leading edge. The microphone located above the leading edge is also used to determine if noise produced at the leading edge significantly contributes to the radiated sound field.

EXPERIMENTAL METHOD

Acoustic tests were conducted in the anechoic wind tunnel at the University of Adelaide. The anechoic wind tunnel test chamber is cubic in shape, approximately 8 m^3 in size and has walls that are acoustically treated with foam wedges. The anechoic wind tunnel contains a contraction outlet that is rectangular in cross section and has dimensions of 75 mm $\times$ 275 mm. The maximum flow velocity at the contraction outlet is 40 m/s.

The flat plate used in these experiments has a chord of 200 mm, a span of 450 mm and a thickness of 5 mm. The flat plate trailing edge is wedge shaped with an apex angle of approximately 12°, while its leading edge is semi-circular in shape with a radius of 2.5 mm. The flat plate is secured to its housing using two side plates and this housing is in turn attached to the contraction flange, as shown in Fig. 1. The span of the flat plate extends beyond the width of the contraction outlet to eliminate the noise produced by the interaction of the flow with the side plates. The anechoic wind tunnel facility, the flat plate and the contraction outlet are shown in Fig. 2.

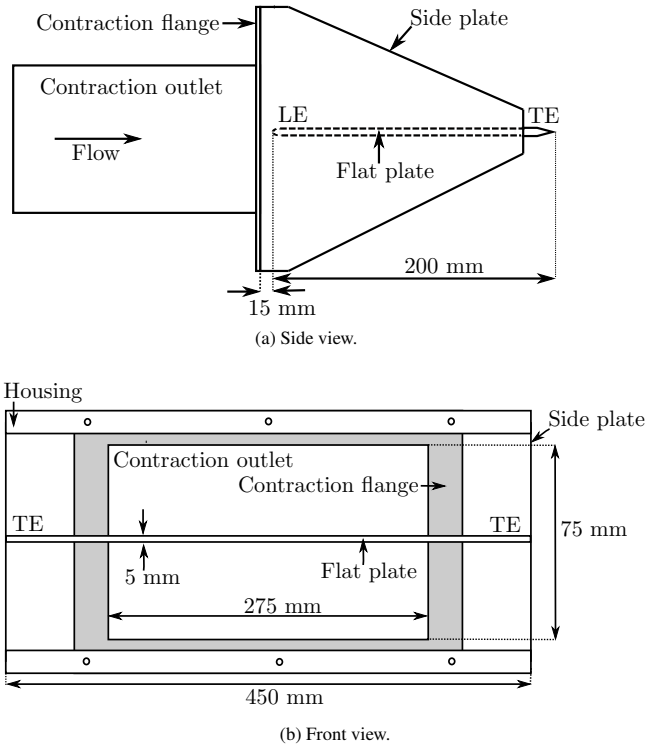

Figure 1: Schematic diagram of the flat plate and the contraction outlet.

Four microphones manufactured by BSWA Technology (Model MP 205) were located in the anechoic wind tunnel: one above, one below and one adjacent to the trailing edge and also one above the leading edge. The top and bottom trailing edge microphones were located at the same radial distance from the trailing edge, perpendicular to the direction of the flow. The positions

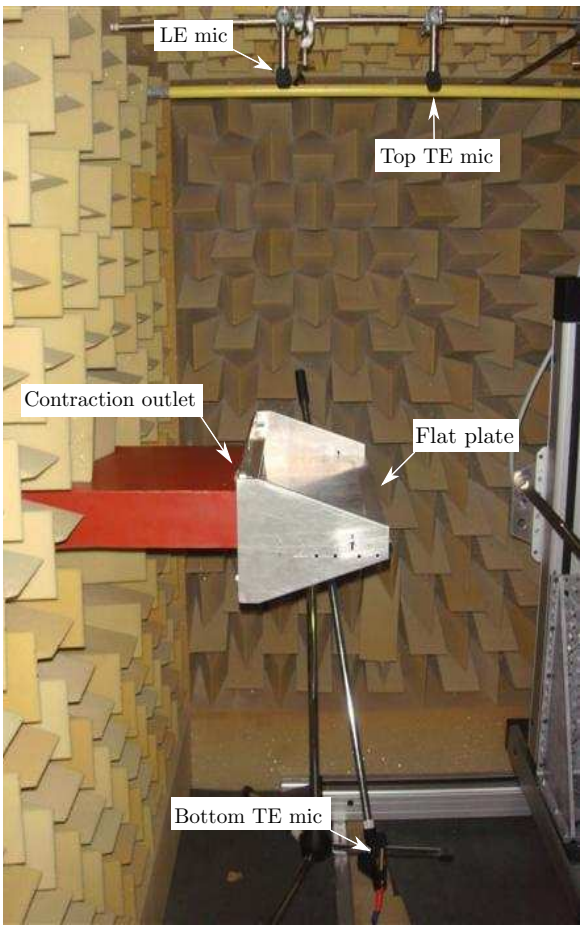

Figure 2: The anechoic wind tunnel facility with the flat plate and the microphones. The side microphone, which is not shown, was located adjacent to the flat plate trailing edge.

of the four microphones are shown in Fig. 3. Each of the four microphones were calibrated before commencing the acoustic tests. To provide isolation from wind noise, wind socks were placed on all four microphones prior to data collection. The microphone data were collected using a National Instruments board at a sampling frequency of 50 kHz for a sample time of 16 s. The presented data have a frequency resolution of 0.0625 Hz.

Experiments were performed at two (plate) angles of attack: $\alpha = 0°$ and $\alpha = 0.5°$. Acoustic measurements were taken at two flow velocities, $v = 38$ m/s and $v = 30$ m/s, corresponding to Reynolds numbers of about 500,000 and 400,000 respectively. For the leading edge microphone and the side microphone, results are presented at the two angles of attack and at a flow velocity of $v = 38$ m/s only, for brevity.

EXPERIMENTAL RESULTS AND DISCUSSION

Acoustic spectra of the top and bottom trailing edge microphone signals and the difference between these two signals are compared with background noise spectra in Fig. 4 for angles of attack of $\alpha = 0°$ and $\alpha = 0.5°$ and flow velocities of $v = 38$ m/s and $v = 30$ m/s. The background noise here is that measured by the top trailing edge microphone. In each case, the spectra measured at the microphones located above and below the trailing edge are of equal magnitude and sit well above the background noise level, especially at lower frequencies. The spectra of the difference between the two microphone signals measured above and below the trailing edge is increased almost

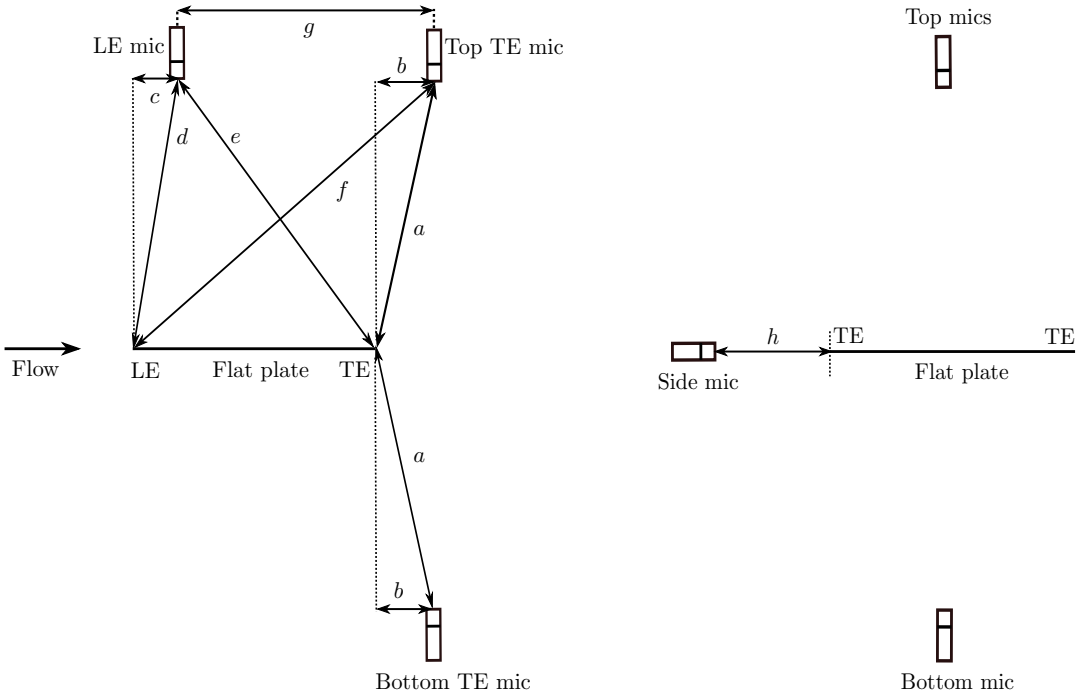

(a) Side view.

(b) Front view.

Figure 3: Microphone positions relative to the flat plate. For $\alpha = 0°$: $a = 0.566$ m, $b = 0.08$ m, $c = 0.06$ m, $d = 0.553$ m, $e = 0.583$ m, $f = 0.622$ m, $g = 0.238$ m and $h = 0.165$ m. For $\alpha = 0.5°$: $a = 0.565$ m, $b = 0.08$ m, $c = 0.06$ m, $d = 0.553$ m, $e = 0.583$ m, $f = 0.620$ m, $g = 0.235$ m and $h = 0.165$ m. The side microphone is not shown in (a) but was located in line with the flat plate trailing edge. Top mics in (b) refers to both the leading edge microphone and the top trailing edge microphone.

6 dB above the spectra of noise measured at a single trailing edge microphone across the entire frequency range. This is because the noise radiated above and below the trailing edge is equal in magnitude, well correlated and out of phase. The phase difference between the signals measured at the top and bottom trailing edge microphones, for both angles of attack and both flow velocities is shown in Fig. 5. This figure confirms that the phase difference between the signals measured above and below the trailing edge is approximately 180° across all frequencies.

The characteristics of trailing edge noise identified by Allen et al. (2002), namely that the sound radiated to opposite sides of the airfoil is well correlated, has equal magnitude and a phase difference of 180°, are clearly displayed in the experimental data presented here. The noise spectra measured above and below the airfoil trailing edge (shown in Fig. 4) are much higher above background noise levels than the isolated trailing edge noise presented in the study by Allen et al. (2002). Also, the noise radiated above and below the trailing edge exhibits much clearer and definite out of phase behaviour than that measured by Allen et al. (2002). This indicates that trailing edge noise was not the dominant noise mechanism at all frequencies in the study by Allen et al. (2002). It is worth noting that Allen et al. (2002) only measured the radiated noise field over the frequency range of 10 to 2000 Hz and that good results of isolated trailing edge noise would not be expected over such a low frequency range.

Changing the angle of attack from by 0.5° has very little effect on the radiated sound field at both flow velocities. This is observed by comparing the spectra in parts (a) and (b) of Fig. 4 to the spectra in parts (c) and (d). Increasing the flow velocity from $v = 30$ m/s to $v = 38$ m/s has the expected affect of slightly increasing the radiated noise levels and this is particularly evident at low frequencies. This result is observed by comparing the spectra in parts (a) and (c) of Fig. 4 to the spectra in parts (b) and (d).

Like trailing edge noise, sound produced at the leading edge and radiated to opposite sides of the airfoil would be well correlated, equal in magnitude and 180° out of phase. Brooks and Marcolini (1985) experimentally analysed the cross-correlation of noise measured above the leading and trailing edge of a flat plate, and showed that noise produced at the leading edge dominated the radiated sound field. It was suggested that the leading edge noise was caused by the interaction of the turbulent boundary layer produced at the test rig's side plates, with the sharp leading edge. To determine whether leading edge noise significantly contributes to radiated sound field in the present study, the top trailing edge microphone signal cross-correlated with the leading edge microphone signal is given in Fig. 6. Microphone signals here have been bandpassed between 800 and 10^4 Hz.

For zero angle of attack, the time delays between sound radiated to the top trailing edge microphone and the leading edge microphone from the trailing edge and leading edge respectively are as follows:

$$\Delta t_{TE} = \frac{(a-e)}{c_0} = \frac{(0.566-0.583)}{c_0} = -4.9\times10^{-5}\text{s}, \quad (1)$$

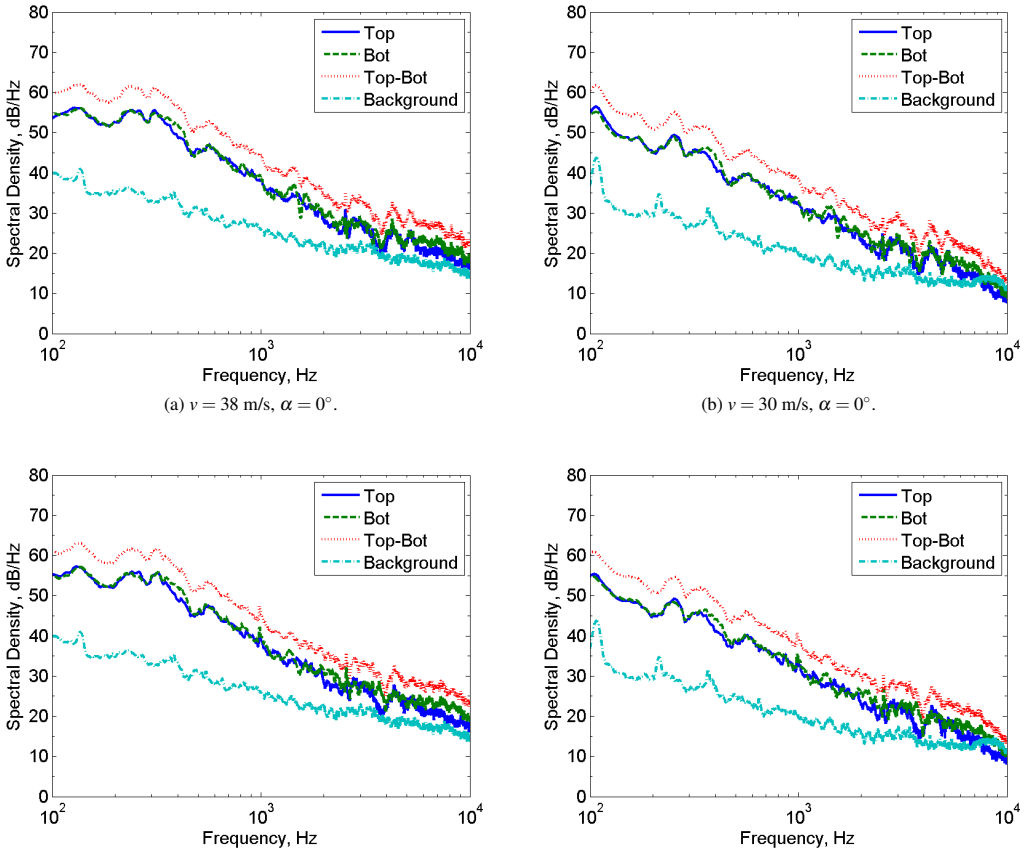

(a) $v = 38$ m/s, $\alpha = 0°$. (b) $v = 30$ m/s, $\alpha = 0°$.

(c) $v = 38$ m/s, $\alpha = 0.5°$. (d) $v = 30$ m/s, $\alpha = 0.5°$.

Figure 4: Acoustic spectra of the top (Top) and bottom (Bot) trailing edge microphone signals and the difference between these two signals (Top-Bot) compared to background (Background) noise spectra. Background noise spectra were measured with the top trailing edge microphone.

and

$$\Delta t_{LE} = \frac{(f-d)}{c_0} = \frac{(0.622-0.553)}{c_0} = 1.9\times10^{-4}\text{s}, \quad (2)$$

where Δt_{TE} is the time delay between sound radiated to the top trailing edge microphone and the leading edge microphone from the trailing edge, Δt_{LE} is the time delay between sound radiated to the top trailing edge microphone and the leading microphone from the leading edge and c_0 is the speed of sound. Values for the lengths a, e, d and f are given in the caption of Fig. 3. For $\alpha = 0.5°$,

$$\Delta t_{TE} = \frac{(a-e)}{c_0} = \frac{(0.565-0.583)}{c_0} = -5.2\times10^{-5}\text{s}, \quad (3)$$

and

$$\Delta t_{LE} = \frac{(f-d)}{c_0} = \frac{(0.620-0.553)}{c_0} = 1.9\times10^{-4}\text{s}. \quad (4)$$

Two peaks are observed in the cross-correlation function at times very close to Δt_{TE} and Δt_{LE} in Fig. 6. This indicates that both trailing edge noise and leading edge noise contribute to the radiated sound field. The magnitude of the cross-correlation function is however, significantly greater at Δt_{TE} than at Δt_{LE}, suggesting that trailing edge noise is the dominant noise mechanism. In these experiments, the span of the flat plate extends beyond the width of the contraction outlet to reduce the interaction of the flow with the side plates. The fact that trailing edge noise dominates the radiated sound field in this case, supports the hypothesis of Brooks and Marcolini (1985), that the leading edge noise is produced by the turbulent boundary layer at the test rig's side plates interacting with the sharp leading edge.

Acoustic spectra of the top and bottom trailing edge microphone signals, the leading edge microphone signal and the difference between any two of these signals are shown in Fig. 7, for $\alpha = 0°$ and $\alpha = 0.5°$ and $v = 38$ m/s. For each angle of attack, the spectra of the leading edge microphone signal is comparable in magnitude to that of the top and bottom trailing edge microphones. This is a result of the leading edge microphone being almost the same distance from the trailing edge as the trailing edge microphones. The amplitude of the spectra of the difference between the signals measured above the leading edge and the trailing edge is significantly less than that of any single microphone. This is because the sound field radiated to the leading edge microphone and the top trailing edge microphone is in phase as both of these microphones are located in the same half plane above the flat plate. The phase difference between the signals measured above the leading edge and the trailing edge is shown in Fig. 8 (a) and (c). These figures confirm that the radiated sound field is largely in phase in the half plane above the flat plate, especially at low frequencies. The phase difference diverges from 0° at high frequencies because the distances from the trailing edge of leading edge and trailing edge microphones differ. The amplitude of the spectra of the difference between the signals measured above the leading edge and below the trailing edge is higher than that of any single microphone and comparable to the spectra of the difference between the signals measured above and below the trailing edge, as shown in Fig. 7. This indicates that the radiated sound field is well correlated and out of phase at the leading edge microphone and the bot-

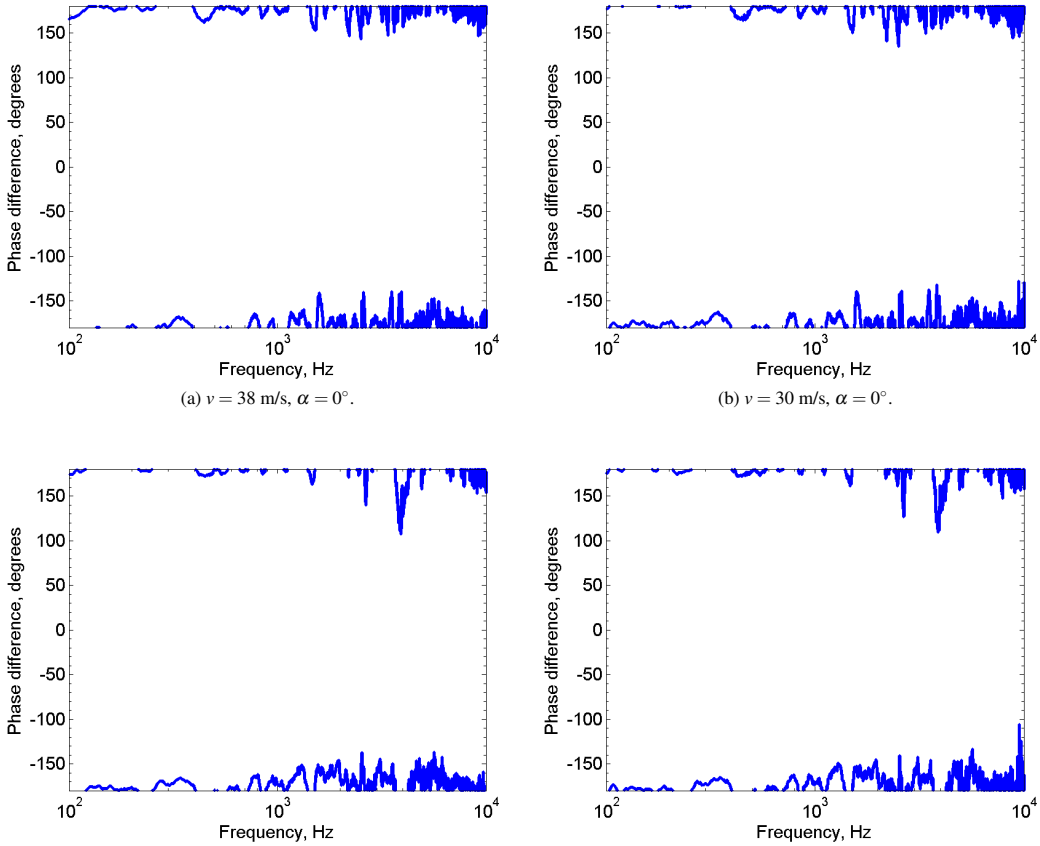

(a) $v = 38$ m/s, $\alpha = 0°$. (b) $v = 30$ m/s, $\alpha = 0°$.

(c) $v = 38$ m/s, $\alpha = 0.5°$. (d) $v = 30$ m/s, $\alpha = 0.5°$.

Figure 5: Phase difference between the signals measured at the top and bottom trailing edge microphones.

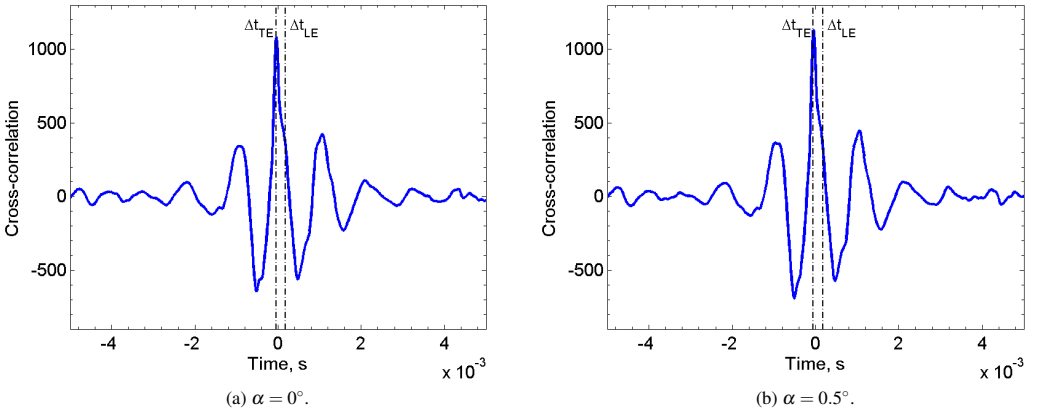

(a) $\alpha = 0°$. (b) $\alpha = 0.5°$.

Figure 6: Cross-correlation between the top trailing edge microphone signal and the leading edge microphone signal for $v = 38$ m/s. Microphone signals have been bandpassed between 800 and 10^4 Hz. The time delays between sound radiated to the top trailing edge microphone and the leading edge microphone from the trailing edge, Δt_{TE}, and the leading edge, Δt_{LE}, are shown with black dash-dot lines. Values for Δt_{TE} and Δt_{LE} are calculated from geometry in Eqns. 1- 4.

tom trailing edge microphone. Fig. 8 (b) and (d) confirm that the phase difference between the signals measured above the leading edge and below the trailing edge is approximately 180° at low frequencies. This 180° phase difference is not observed at high frequencies because the leading edge and trailing edge microphones are slightly different distances from the trailing edge.

Acoustic spectra of the top and bottom trailing edge microphone signals, the difference between these two signals and the side microphone signal are shown in Fig. 9, for $\alpha = 0°$ and $\alpha = 0.5°$ and for $v = 38$ m/s. For both angles of attack, noise levels measured adjacent to the trailing edge are significantly less than that of the top and bottom trailing edge microphones. As expected, this suggests that significantly more trailing edge noise is radiated above and below the flat plate than adjacent to it. This is especially significant given that the side microphone had to be located much closer to the trailing edge than the microphones above and below due to space restrictions. The phase difference between the side microphone and the top and

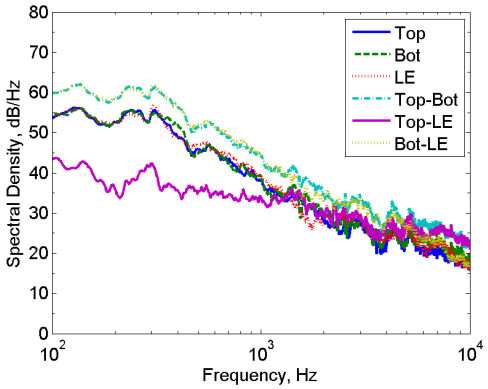

(a) $\alpha = 0°$.

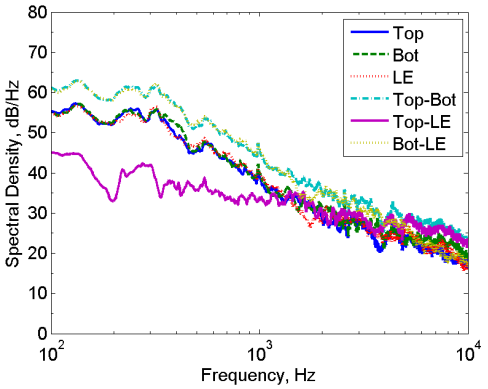

(b) $\alpha = 0°$.

Figure 7: Acoustic spectra of the top (Top) and bottom (Bot) trailing edge microphone signals, the leading edge (LE) microphone signal and the difference between any two of these signals (Top-Bot, Top-LE, Bot-LE) for $v = 38$ m/s.

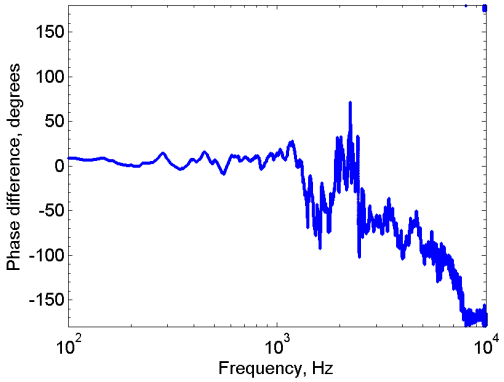

(a) Top TE microphone and LE microphone, $\alpha = 0°$.

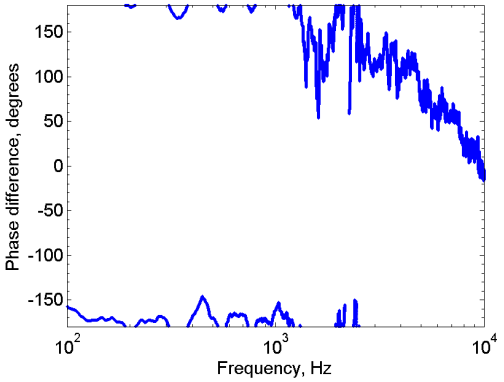

(b) Bottom TE microphone and LE microphone, $\alpha = 0°$.

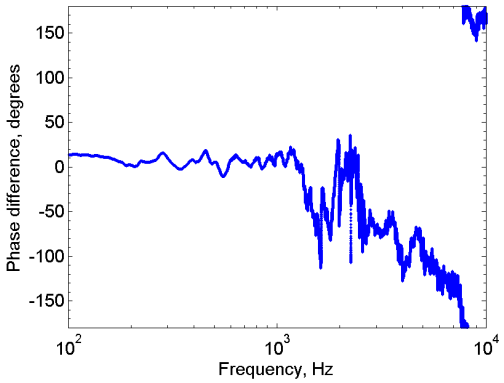

(c) Top TE microphone and LE microphone, $\alpha = 0.5°$.

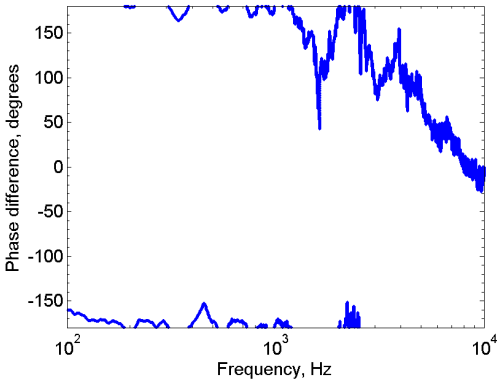

(d) Bottom TE microphone and LE microphone, $\alpha = 0.5°$.

Figure 8: Phase difference between the signals measured at the leading edge (LE) microphone and the top and bottom trailing edge (TE) microphones for $v = 38$ m/s.

bottom trailing edge microphones for $\alpha = 0°$ and $\alpha = 0.5°$ and for $v = 38$ m/s is shown in Fig. 10. It is observed that the noise radiating to the side microphone exhibits steadily increasing phase behaviour with respect to noise measured above or below the trailing edge, consistent with the understanding of the noise field.

CONCLUSION

Trailing edge noise radiated into the far-field from a flat plate airfoil encountering smooth fluid flow has been experimentally analysed in this paper. Far-field noise spectra were measured at four microphone locations and information about the directivity of the trailing edge noise was ascertained by comparing the four microphone signals. A method for extracting and analysing trailing edge noise by combining the work of Brooks and Marcolini (1985) and Allen et al. (2002) has been presented here. As found in the study by Allen et al. (2002), trailing edge noise radiated to microphones above and below the trailing edge was seen to be well correlated, of equal magnitude and to have a phase difference of 180°. Comparison with data from a micro-

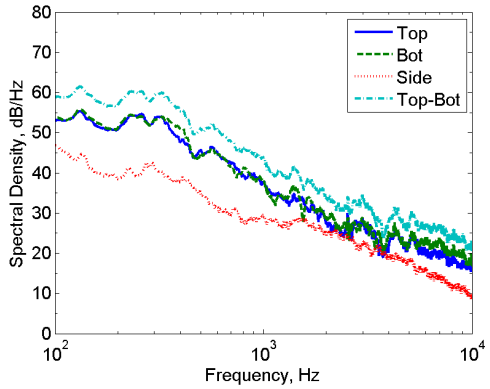

(a) $\alpha = 0°$.

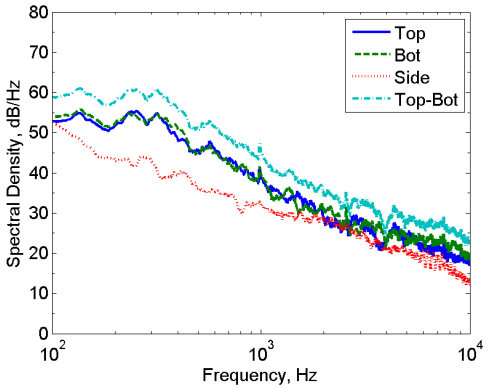

(b) $\alpha = 0°$.

Figure 9: Acoustic spectra of the top (Top) and bottom (Bot) trailing edge microphone signals, the difference between these two signals (Top-Bot) and the side (Side) microphone signal for $v = 38$ m/s.

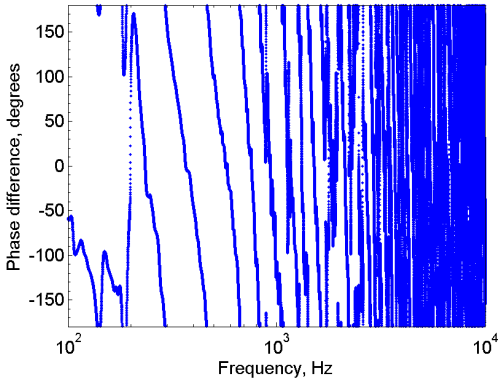

(a) Top TE microphone and side microphone, $\alpha = 0°$.

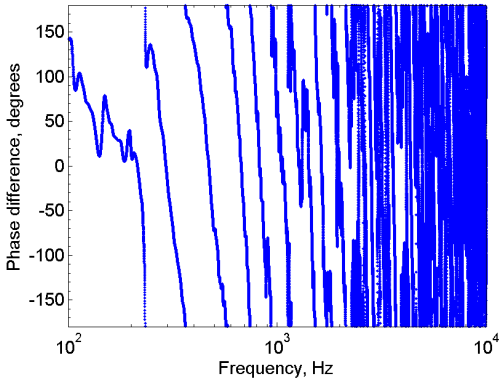

(b) Bottom TE microphone and side microphone, $\alpha = 0°$.

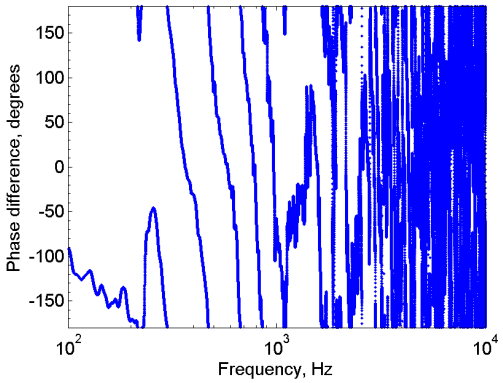

(c) Top TE microphone and side microphone, $\alpha = 0.5°$.

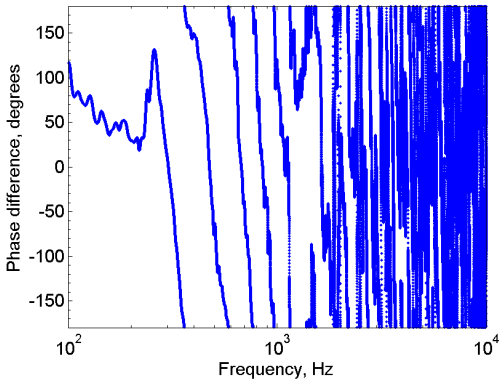

(d) Bottom TE microphone and side microphone, $\alpha = 0.5°$.

Figure 10: Phase difference between the signals measured at the side microphone and the top and bottom trailing edge (TE) microphones for $v = 38$ m/s.

phone above the leading edge demonstrated that noise radiating from the leading edge contributed to the radiated noise field but was not the dominant airfoil self-noise mechanism. Subtracting the out-of-phase signals measured above and below the trailing edge was shown to increase the airfoil trailing edge noise spectra further above that of the ambient noise. It should be noted that an offset value of 6 dB needs to be subtracted from this trailing edge noise spectra when using this method for isolating the trailing edge noise. Noise measured adjacent to the trailing edge was found to be significantly lower in amplitude than that measured above or below the trailing edge as expected. The high quality of these experimental results demonstrates the effectiveness of measuring trailing edge noise in the anechoic wind tunnel facility.

The experimental investigation detailed in this paper is the first in a series of experimental tests to measure trailing edge turbulent flow and far-field noise data for different airfoil shapes and flow conditions. It is planned that experimental measurement of simultaneous flow and acoustic data will be performed in the wind tunnel at the University of Adelaide. Far-field acoustic measurements will be made using point and array tech-

niques while flow data, including Reynolds stress contour maps about the airfoil trailing edge, will be measured using hot-wire anemometry. The results of this comprehensive experimental study will aid understanding of the trailing edge noise mechanism and will be used for validating theoretical noise predictions calculated using computational aeroacoustic techniques such as LES.

ACKNOWLEDGEMENTS

This work has been supported by the Australian Research Council under grant DP1094015 'The mechanics of quiet airfoils'. The authors gratefully acknowledge their support.

REFERENCES

C.S. Allen, W.K. Blake, R.P. Dougherty, D. Lynch, P.T. Soderman, and J.R. Underbrink. *Aeroacoustic measurements*. Springer, 2002.

R.K. Amiet. Noise due to turbulent flow past a trailing edge. *Journal of Sound and Vibration*, 47(3):387–393, 1976.

W.K. Blake. *Mechanics of Flow Induced Sound and Vibration*, volume I and II. Academic Press, London, UK, 1986.

T.F. Brooks and T.H. Hodgson. Trailing edge noise prediction from measured surface pressures. *Journal of Sound and Vibration*, 78(1):69–117, 1981.

T.F. Brooks and M.A. Marcolini. Scaling of airfoil self-noise using measured flow parameters. *AIAA Journal*, 23(2): 207–213, 1985.

T.F. Brooks, S. Pope, and M.A Marcolini. Airfoil self-noise and prediction. Technical report, NASA Reference Publication 1218, 1989.

K.L. Chandiramani. Diffraction of evanescent waves with applications to aerodynamically scattered sound and radiation from unbaffled plates. *Journal of the Acoustical Society of America*, 55:19–29, 1974.

D.M. Chase. Noise radiated from an edge in turbulent flow. *AIAA Journal*, 13:1041–1047, 1975.

C.J. Doolan. A review of airfoil trailing edge noise and its prediction. *Acoustics Australia*, 1:7–13, 2008.

X. Gloerfelt and T. Le Garrec. Trailing edge noise from an isolated airfoil at a high reynolds number. In *15th AIAA/CEAS Aeroacoustics Conference*, Miami, Florida, 11-13 May 2009.

M.S. Howe. A review of the theory of trailing edge noise. *Journal and Sound and Vibration*, 61(3):437–465, 1978.

Y. Khalighi, A. Mani, F. Ham, and P. Moin. Prediction of sound generated by complex flows at low mach numbers. *AIAA Journal*, 48(2):306–316, 2010.

C. Kunze. Acoustic and velocity measurements in the flow past an airfoil trailing edge. Master's thesis, Aerospace and Mechanical Engineering, University of Notre Dame, Indiana, 2004.

C. Kunze, D.A. Lynch, and T.J. Mueller. Effect of trailing edge geometry on vortex shedding and acoustic radiation. In *8th AIAA/CEAS Aeroacoustics Conference*, Breckenridge, Colorado, 17-19 June 2002.

D.P. Lockard and G.M. Lilley. The airframe noise reduction challenge. Technical Report NASA/TM-2004-213013, NASA, 2004.

S. Oerlemans, M. Fisher, T. Maeder, and K. Kogler. Reduction of wind turbine noise using optimized airfoils and trailing-edge serrations. *AIAA Journal*, 47(6):1470–1481, 2009.

M. Roger and S. Moreau. Broadband self-noise from loaded fan blades. *AIAA Journal*, 42(3):536–544, 2004.

R.H. Schlinker and R.K. Amiet. Helicopter rotor trailing edge noise. Technical Report NASA Contractor Report No. 3470, NASA, 1981.

M. Wang and P. Moin. Computation of trailing-edge flow and noise using large-eddy simulation. *AIAA Journal*, 38(12): 2201–2209, 2000.

J. Winkler, S. Moreau, and T. Carolus. Large-eddy simulation and trailing-edge noise prediction of an airfoil with boundary-layer tripping. In *15th AIAA/CEAS Conference*, Miami, Florida, 11-13 May 2009.